International Journal of Engineering and Information Systems (IJEAIS)
ISSN: 2643-640X
Vol. 4, Issue 8, August – 2020, Pages: 241-251

Single-End Measuring Scheme for Open Conductor Fault Detection Based on Discrete Wavelet Transform in HV Transmission Lines

Basem Abd-Elhamed Rashad[1], Doaa K. Ibrahim[2], Mahmoud I. Gilany[3], Aboul'fotouh El'gharably[4]
[1]Electrical Power & Machines Department, The Higher Institute of Engineering at El-Shorouk City, Cairo, Egypt
eng_basemabdelhamed@yahoo.com
[2]Electrical Power Engineering Department, Faculty of Engineering, Cairo University, Cairo, Egypt
[3]Electrical Power Engineering Department, Faculty of Engineering, Cairo University, Cairo, Egypt
[4]Electrical Power & Machines Department, The Higher Institute of Engineering at El-Shorouk City, Cairo, Egypt

Abstract*—*This article provides a novel adaptive single-end measuring scheme to identify (detect and classify) faults in HV transmission systems using Discrete Wavelet Transform. Fault identification scheme is sensitive and automated for solving the present challenges such as high-impedance faults (HIFs) and open conductor fault (OCF). The proposed scheme unit (PSU) estimates the threshold values adaptively according to the pre-fault value of wavelet decomposed current approximation coefficient. Comprehensive EMTP / ATP simulations are used to evaluate PSU performance. PSU is investigated with various faults types, different locations, and different fault resistance and inception angles on a 500 kV, 350 km transmission line. The simulation results have shown that the PSU can detect OCFs, LIFs and HIFs correctly, using one end current signals. The results demonstrate that the PSU is fast, robust, precise and reliable.

Keywords—Discrete Wavelet Transform (DWT), HV Transmission Lines, Fault identification scheme, Transient-based protection

1. INTRODUCTION

Transmission lines protection is a vital requirement in power system operation and thus every possible measure is taken in this regard. Protection of the transmission lines is a challenge in identifying and isolating faults that accurately impact the power system security. Mal-operation of protective devices in detecting faults and eliminating the disturbance effects during faulty period may cause instability in power system [1].

Faults of Transmission lines can be classified into two main types according to their nature: faults with low-impedance (LIFs) and faults with high-impedance (HIFs), while HIFs contain open conductor faults (OCFs). LIFs include single line-to-ground (SLG) faults, line-to-line (L-L) faults, etc., Actually OCFs are dangerous since public is posed to the risks of electric shocks and the fire hazard also exists. In fact, detection of OCF is still a challenge due to its very low fault current value which is not detected through conventional primary protection devices [2].

Causes of OCFs on transmission lines (TL) include undesired opening of breaker operation (one-pole opening), case of open bridle (especially in tension towers) and line conductor direct breaking. Opening a conductor in power TL is a big problem in the operation of power systems; and has a harmful impact on the system stability as the system operates on two phases only, the transmitted power is reduced through the line and the healthy phases can suffer from overload. Therefore, the voltage upon healthy phases may increase if the system is not directly earthed [3]. OCFs may not be detected by primary protection of the TL distance relay as a significant current increase or a voltage reduction is not associated with an OCF. This open conductor fault (OCFs) will continue until it is detected by another protection system.

Several papers have been published for TL fault identification using several WT applications such as DWT, wavelet packet transform (WPT) and wavelet single entropy (WSE). Several reported methods utilized the DWT as an effective tool for analysing the fault transients to extract the frequency and time domain information during HIFs [4, 5]. The algorithm such as reported in [6] presented a review study about fault identification schemes for transmission networks, whereas, the main issue is how the high-frequency component is extracted from the faulty signal.

The fault detection in TL based on WT and Discrete Fourier Transform (DFT) methods is reported in Refs. [7]. In Ref. [8], a fault detection technique is introduced based on the instantaneous RMS values of powers from both ends of the TL, the scheme takes long than 20 ms to determine RMS value. In Ref. [9] the average time for fault detection is 20 ms, depending on the multi-resolution S-transform and probabilistic artificial neural network (ANN).

In [10], a protection algorithm based on wavelet coefficients of the transient current signal is presented with fast fault detection, the fault detection time is 20 ms. Ref. [11] presented an approach that combines the WSE theory and fuzzy logic with fast fault

detection time about 20 ms. Ref. [12] presented an approach that combines the intelligent traveling-wave (TW) and fuzzy logic system to locate the internal faults with fast fault detection time.

Out of the various techniques reported for HV transmission lines protection, few of them have been applied for the protection against OCFs [13, 14]. The used techniques include utilizing negative sequence components for series and shunt faults protection as described in [13]. A protection scheme based on Fuzzy inference system for OCFs in three phase transmission system has also been developed in [14]. Actually, the reliability of intelligent techniques based protection scheme is highly influenced by its architecture selection and training.

In this approach, individual phase current waveforms are analysed based on discrete wavelet transform (DWT) method which has perfect time–frequency localization ability. This article presents a new single-end adaptive measurement scheme which utilized DWT to current signals to detect and classify all faults in HV transmission systems. The technique can be applied to different network configurations including double end lines without synchronization or communication between the two ends. In general, PSU is independent on tested system parameters and their variation. Moreover, it avoids the need for extensive series of system studies to calculate the optimal threshold value.

2. OVERVIEW ON THE FAULT IDENTIFICATION SCHEME

As stated previously, the objective of the proposed scheme is to detect and classify all types of faults. Fig.1 illustrates the fault types. It includes:

- Open conductor from two sides (OCFTS), as shown in (Fig. 2-a). This fault may occur when the bridle wire is cut and suspended from both sides without touching the tower as shown in (Fig. 2-b).
- Simplified two-diodes model for HIFs, as shown in (Fig. 2-c).
- Simplified Low Impedance Fault model, as shown in (Fig. 2-d).

The proposed scheme unit (PSU) adaptively detects LIFs, HIFs and OCFs based on DWT without using any additional classifier technique. In particular, single-level DWT decomposition with a sampling rate of 200 kHz (4000 samples per cycle at 50 Hz) is used in the proposed scheme for a fault identification scheme. It uses high- frequency and low-frequency components to improve discrimination between various types of faults.

2.1 Discreet Wavelet Transform (DWT)

A non-stationary signal analysis using the Fourier Transform (FT) or the Short Time Fourier Transform (STFT) does not provide satisfactory results. Accurate results can be obtained using wavelet analysis. The most important issues of wavelet analysis is the ability to perform local analysis, and able to reveal signal aspects that other analysis techniques fail. Wavelet analysis makes it possible to perform a multi-resolution analysis as compared to the STFT [15].

In this regard, Discrete Wavelet Transform (DWT) is used. Recursively filtering the signal with a high and low-pass filter. The output of high-pass filter is known as the detail coefficients, which are the high-frequency, low-scale signal components, and the output of low-pass filter is known as the approximate coefficients, which are the low-frequency, high-scale signal components. Cascading procedures is applied to acquire another level of decomposition, Wavelet coefficients can mathematically be determined accordingly [7]:

where, $CA1[K]$ and $CD1[K]$ are the coefficients of wavelet decomposition which analysing signal at level 1, The coefficients also yield with the initialize of the mother wavelet implemented.

$$CA1[K] = \sum_{n=-\infty}^{n=\infty} X[n] * L[2K - n] \qquad (1)$$

$$CD1[K] = \sum_{n=-\infty}^{n=\infty} X[n] * h[2K - n] \qquad (2)$$

International Journal of Engineering and Information Systems (IJEAIS)
ISSN: 2643-640X
Vol. 4, Issue 8, August – 2020, Pages: 241-251

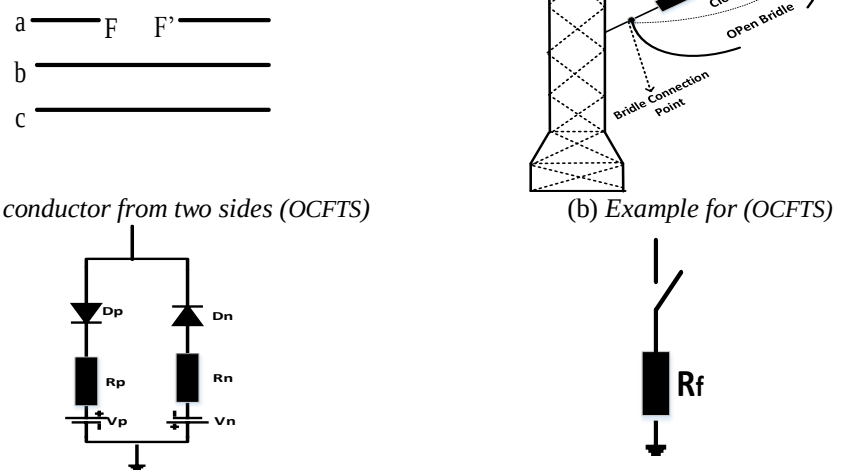

(a) *Open conductor from two sides (OCFTS)* (b) *Example for (OCFTS)*

(c) Simplified two-diodes model for HIFs (d) Simplified LIF model

Fig. 1. *Presentation of fault models*

2.2 Mother Wavelet Selection

As a matter of fact, capturing different signals variations using DWT depends mainly on the proper selection of the mother wavelet. The selection depends on the nature of the application for the fault detection. In practice, the shape of the faulted signal is comparing with the utilized wavelet function [15]. Actually, the most suitable mother wavelet for fault detection and classification in PSU should satisfy the following three main conditions:

- A significant magnitude of first level of detailed coefficient for detecting the fault.
- The smallest difference between the reconstructed and the original signals is attained.
- Major variation between faulty phase and healthy phases can be sensed.

According to extensive studies depending on the three aforementioned conditions, the suitable mother wavelet for the proposed scheme unit is db1 for detection procedure. It must be pointed out that as only a single level of decomposition is employed for detection and classification procedure; the computational requirements of PSU are reduced appreciably compared with multilevel decomposition employed in several published works such as [16, 17].

Fig.2 summarizes the overall structure for Fault patterns process. In the following sections, description of the proposed schemes is fully introduced.

2.3 Proposed Identification Scheme

In the proposed identification procedure, which includes detection and classification procedure, the wavelet decomposed current approximation and detail coefficients for the three-phase current (ia, b, c) and the ground current (ig) signals are considered to perfectly detect and classify the fault cases.

The algorithm procedure for detection and classification aims at:

- The three-phase signals $(ia, ib \ and \ ic)$, and ground current signal (ig), where $ig = (ia + ib + ic)$, are decomposed using ***db1*** to get high-frequency components and low-frequency components based on equations (1) & (2) respectively.

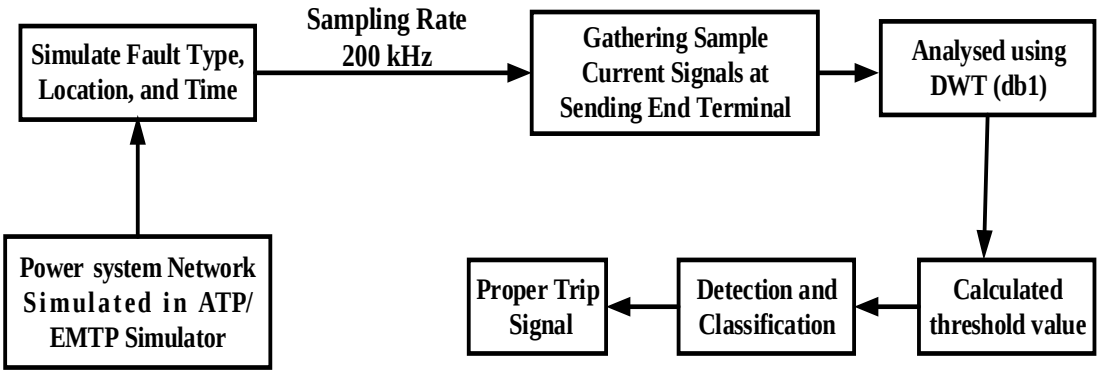

Fig. 2. *Overall structure for Fault patterns process*

- After decomposing the maximum absolute values for current approximation coefficient for the three-phase current and the ground current signals (Ma,Mb, Mc and Mg) are calculated. For ground faults classification the ground current approximation is used
- Estimate the absolute sum for current detail coefficients (Sa, Sb and Sc) of the decomposed currents, and then the differences of the sum absolute value for current detail coefficients (Ha, Hb and Hc) are evaluated as: $Ha = |Sa - Sb|$, $Hb = |Sb - Sc|$, $Hc = |Sc - Sa|$.
- The approximation coefficients ratios (Ra, Rb and Rc) are calculated as: $Ra = |Ma/Mb|$, $Rb = |Mb/Mc|$, $Rc = |Mc/Ma|$. These ratios are used as detection parameters in case of HIFs including OCFs.
- **Finally,** for accurate Discrimination between LIFs, HIFs and OCFs by applying the following conditions:
  - LIF is confirmed if :
    - $Ma > Mth$ or $Mb > Mth$ or $Mc > Mth$ is fulfilled. Only the M-value for the faulty phases will exceed the limit.
  - OCF is confirmed if all the following conditions are fulfilled:
    - All the conditions: $Ma < Mth$ & $Mb < Mth$ & $Mc < Mth$ are achieved and,
    - One of the conditions: $Ha > Hth$ or $Hb > Hth$ or $Hc > Hth$, is achieved, and
    - One of the ratios: $Ra > 1$ or $Rb > 1$ or $Rc > 1$, is achieved.
  - HIF is confirmed if all the following conditions for OCF are fulfilled except :
    - All the ratios: $Ra \leq 1$ or $Rb \leq 1$ or $Rc \leq 1$, is achieved.

2.4 Estimation of Threshold Values

The threshold values are calculated adaptively to handle the current variations. The setting for current approximation coefficients are calculated using pre-fault value after first installation and after every normal change in the current values. Consequently, the threshold values utilized in the proposed scheme (Mth and Hth) are calculated as follows:

$$Mth = |(Ma + Mb + Mc)/3| \times C1 \quad (3)$$

$$Hth = |(Mth \times C2)| \quad (4)$$

Where, (Ma,Mb, and Mc) are the maximum absolute values for a wavelet decomposed current approximation coefficient of the three-phase current signals. The value of the coefficients $C1$ and $C2$ is chosen as 1.2 and 0.1 respectively.

$C1$ is selected to accurate discriminate between healthy and faulty phases, in different cases, the healthy phases have small change after a fault occurrence does not exceed 10%. So, for accurate discrimination, a safety margin about 20% is used. Moreover, $C2$ is selected as 5% for higher sensitivity. The adaptive variations in the threshold values are tested in different systems to confirm validity with different topology.

The value of required frequency aspects should stay above threshold value for more than one power frequency cycle (20 ms) to ensure a correct tripping decision. Fig.3 illustrates the complete flowchart of the proposed scheme for detecting the fault.

International Journal of Engineering and Information Systems (IJEAIS)
ISSN: 2643-640X
Vol. 4, Issue 8, August – 2020, Pages: 241-251

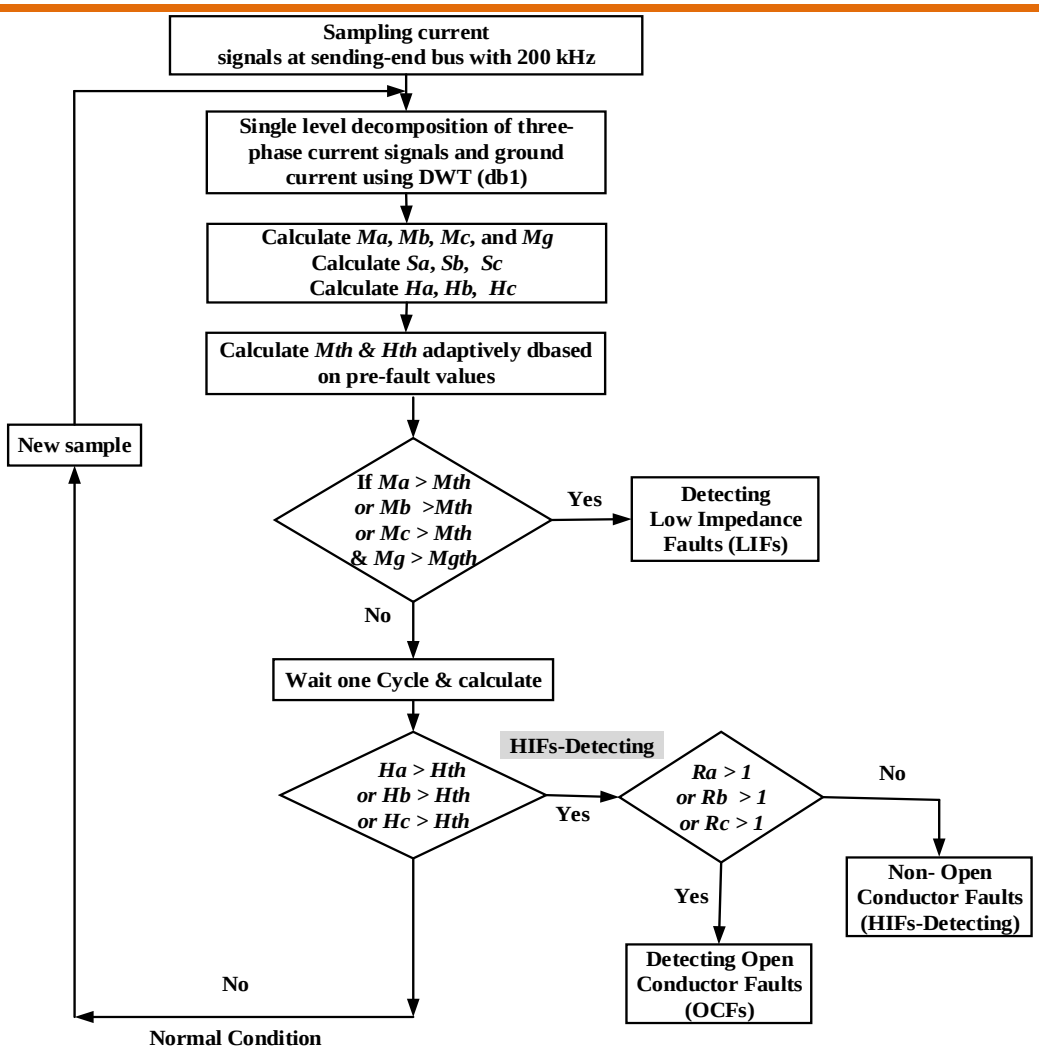

Fig. 3. *Flowchart of The proposed Fault identification scheme*

3. TESTING PROPOSED SCHEME FOR FAULT IDENTIFICATION PROCEDURE

The double-ended 500 kV, 350 km transmission line model is simulated using ATP/EMTP to simulate fault signals at a sampling rate of 200 KHz as shown in Fig.4. The main parameters of the tested system are demonstrated in Table 1. Moreover, the open conductor from two sides is shown in Fig. 1a,while the HIF model is presented based on arcing in sandy soil [18] as shown in Fig. 1c. And finally, The LIF model includes the appropriate fault resistance Rf switched at the fault location in the line is shown in Fig. 1d.

The simulations studies are performed to cover different types of fault patterns including:

- Fault types considered in this work are: single-line-to-ground (SLG), double-line-to-ground (DLG), line-to-line (L–L),three-phase fault (3LG)
- Open conductor from two sides (OCFTS).
- Open conductor from one side followed by earth fault in other side (or vice versa). For these two types, the faulty phase is assumed to be suspended from one end and the other end is earthed after the phase is opened by 0.035 s.
- High Impedance Fault (HIF) based on arcing in sandy soil

- Different fault locations of the protected line.
- Different fault angles on the voltage waveform (varies between 0° and 318°, at regular intervals of 18°).
- Different fault resistance is considered.

International Journal of Engineering and Information Systems (IJEAIS)
ISSN: 2643-640X
Vol. 4, Issue 8, August – 2020, Pages: 241-251

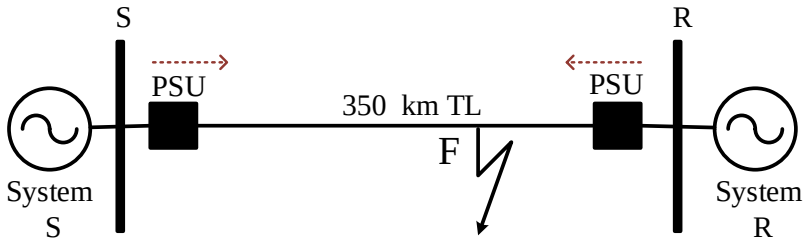

Fig.4. *Single line diagram of tested 500 kV system*

Table 1 Simulated system parameters

System Voltage, Frequency	500 kV, 50 Hz
System Impedance at Sending end bus (S), (δ=0°)	$Z_{L1} = 18 + j43.1749\ \Omega$ $Z_{L0} = 15 + j30.2221\ \Omega$
System Impedance at Receiving end bus (R), (δ= -15°)	$Z_{R1} = 26 + j44.9185\ \Omega$ $Z_{R0} = 20 + j37.4698\ \Omega$
line SR (350 km)	$Z_1 = 0.00758 + j0.26365\ \Omega$ /Km $Z_0 = 0.15421 + j\ 0.8306\ \Omega$ /Km $C_1 = 13.97$ nF/km $C_0 = 9.296$ nF/km

3.1 DISTINGUISHING LOW-IMPEDANCE FAULTS (LIFS)

The system shown in Fig. 4 is used for simulation studies. The measured current from one end of each phase is analysed using DWT to extract the transient features. The current waveforms measured at the PSU at S terminal and current approximation coefficients (Ma, Mb, Mc, Mg) of Line-to-line fault (BC) are shown in Fig.5 (a), while Fig.5 (b) displays the related waveforms of three-phase fault (ABC). The fault in each situation has occurred with a low fault resistance of 15 Ω at 0.04 s and 20 km from PSU.

The scheme accurately classifies the criteria for LIF occurrence. As shown in Fig.5 (a), the achieved relations were: $Mb > Mth$, $Mc > Mth$ and $Mg < Mth$, and thus the fault is properly identified as a fault of BC. Furthermore, as illustrated in Fig.5 (b) which displays that $Ma > Mth$, $Mb > Mth$, $Mc > Mth$ and $Mg < Mth$, this condition is accurately defined as ABC fault. It is therefore clear that LIFs will be correctly discriminated and classified by PSU.

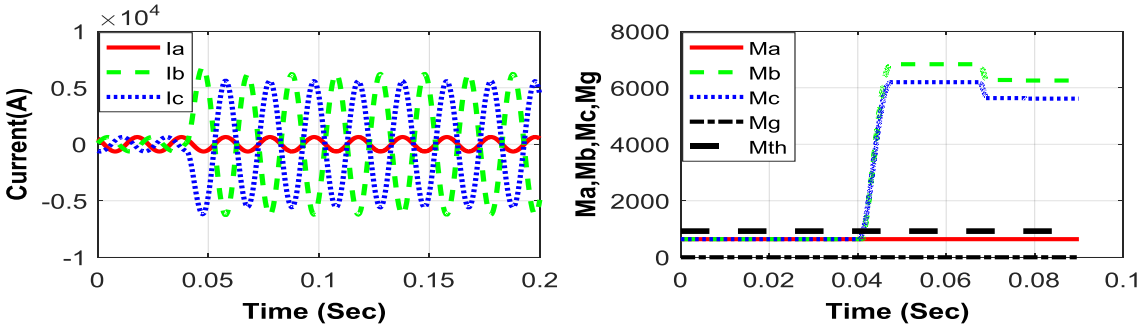

(a) Line-to-line fault (BC)

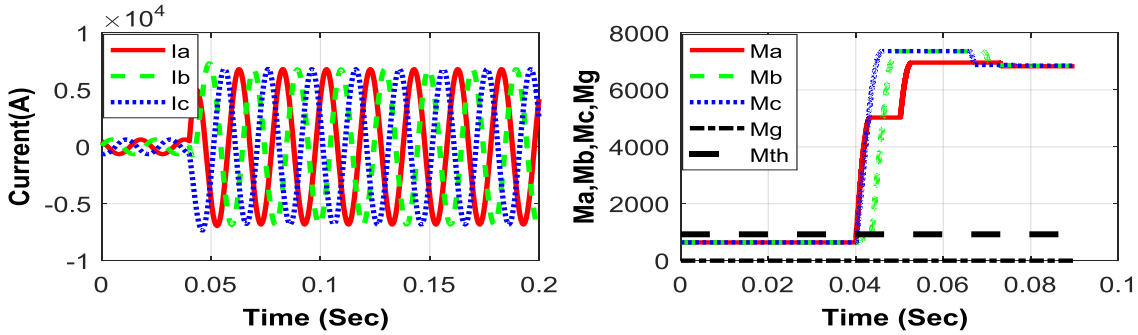

(b) Three-phase fault (ABC)

Fig.5: Measured current waveforms at PSU, and calculated current approximation coefficients (Ma,Mb,Mc,Mg) for LIFs (15 Ω) at 20 km from PSU location at 0.04 s

3.2 DISTINGUISHING OPEN CONDUCTOR FAULTS (OCFS)

The system shown in Fig. 4 is used for simulation studies. The measured current from one end of each phase is analysed using DWT to extract the transient features.

The effectiveness of PSU installed at the beginning of the protected line is evaluated for various simulated OCFs occurring at 20 km from PSU to prove PSU performance in detecting different OCF types. Fig. 6 indicates three different OCFs: Fig.6 (a) represents an OCF on phase A from two sides (OCFTS), Fig.6 (b) represents an OCF on phase A at the relay side where the other end is earthed through a low resistance of 3 ohm (OC/R+EF) and finally Fig. 6 (c) represents an OCF on phase A at the opposite relay side where the terminal at the relay side is earthed through a low resistance of 3 ohm (OC/O+EF).

The current waveforms analyzed at PSU, current approximation coefficients ($Ma, Mb, Mc,$ and Mg), differences of the sum absolute value for current detail coefficients ($Ha, Hb,$ and Hc), and approximation coefficients ratios ($Ra, Rb,$ and Rc) are demonstrated in Fig. 6.

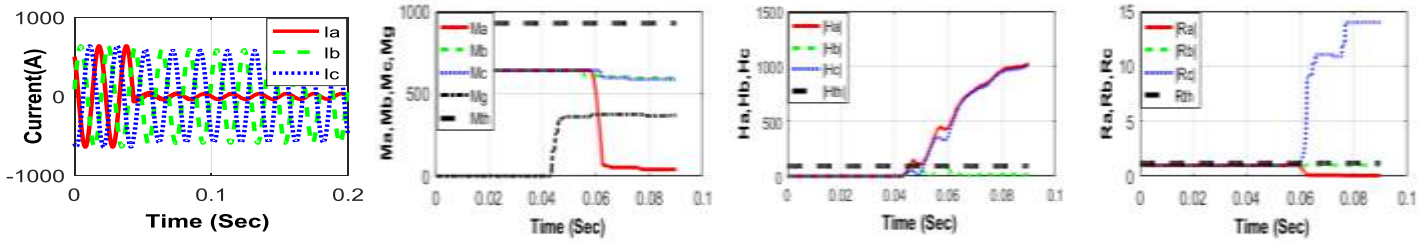

(a) OCFTS (Open conductor on phase A from two sides)

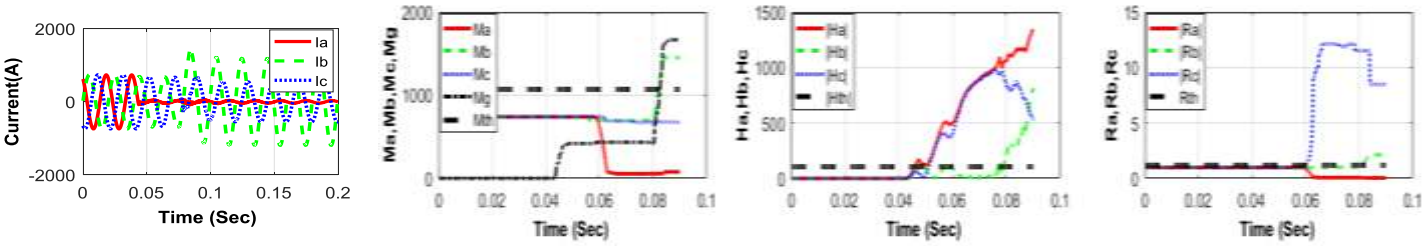

(b) OC/R+EF (Open conductor on Phase A at the relay side where the other side is earthed)

International Journal of Engineering and Information Systems (IJEAIS)
ISSN: 2643-640X
Vol. 4, Issue 8, August – 2020, Pages: 241-251

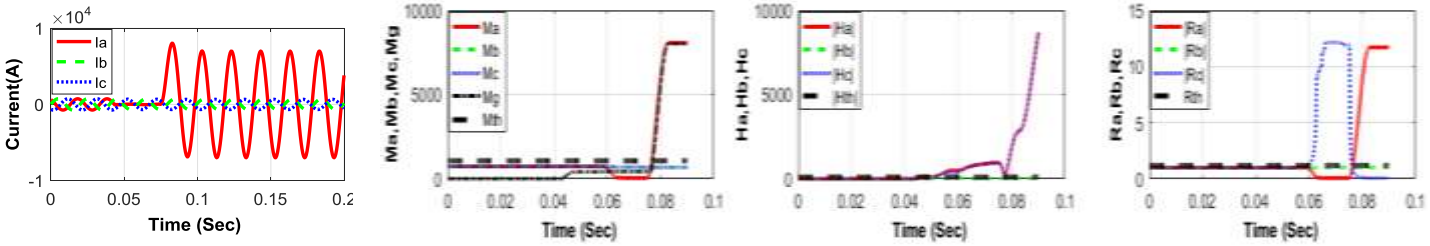

(c) OC/O+EF (Open conductor on Phase A at the opposite relay side where the relay side is earthed)

Fig.6. *measured current waveforms at PSU, calculated current approximation coefficients (Ma,Mb,Mc, Mg), differences of the sum absolute value for current detail coefficients (Ha,Hb,Hc) and approximation coefficients ratios (Ra, Rb, Rc) for different types of OCFs at 20 km from PSU at 0.04 s*

It is obvious from scheme performance in these three simulated different OCFs types that all the three conditions required for recognition of OCFs are fulfilled as follows:

- As seen in Fig.6 (a), 6 (b) and 6 (c) all the M-values ($Ma, Mb, and\ Mc$) are less than the threshold Mth are achieved. However, when one or more of these M-values exceed the threshold Mth upon the instant as seen for M-graphs in Fig.6 (b) and 6 (c), then the other end of the conductor is earthed for both OC/R+EF and OC/O+EF.
- As seen in the H-graphs of Fig.6 (a), 6 (b) and 6 (c), at least one of the H-values (Ha, Hb, and Hc), exceeds the threshold Hth and stays above for more than 1 cycle, is also obtained.
- As seen in the R-graphs of Fig.6 (a), 6 (b) and 6 (c), at least one of the R-values ($Ra, Rb,$ and Rc) exceeds the limit Rth, is also achieved.

As the required conditions are all satisfied, it can be concluded that these particular cases are essentially verified as OCFs using the PSU.

3.3 DISTINGUISHING HIGH IMPEDANCE FAULTS (HIFS)

The system shown in Fig.4 is used for simulation studies. The measured current from one end of each phase is analysed using DWT to extract the transient features. Shunt HIFs are also extensively tested to investigate the effectiveness of the suggested HIF identification scheme. Fig.7 displays the combined measured features used to enhance the detection of HIFs based on low and high-frequency components. Fig.7 (a) depicts a single-line-to-ground HIF where the effects for phase-to-phase HIF are shown in Fig.7 (b).

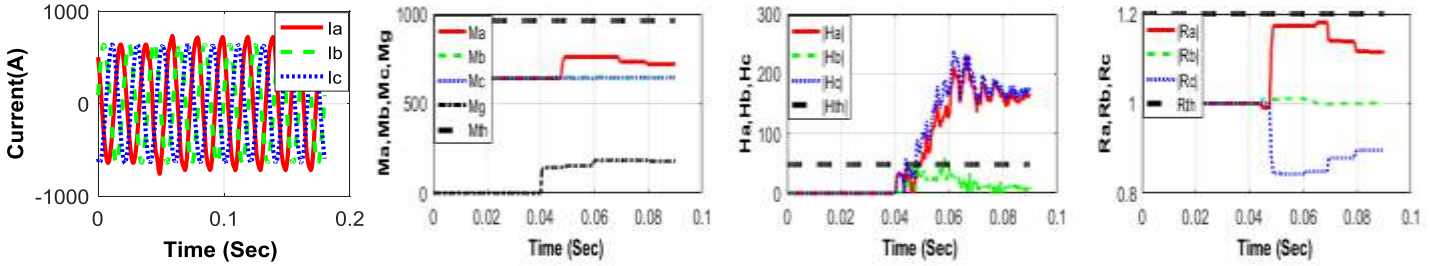

(a) Single-line-to-ground HIF

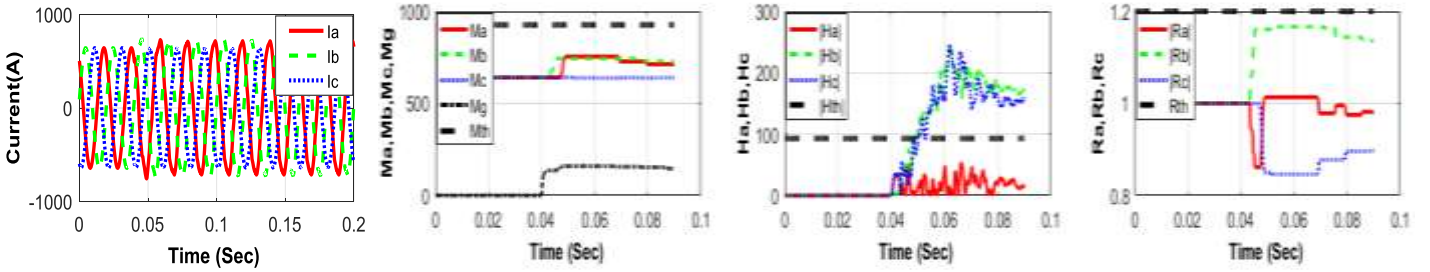

(b) Phase-to-phase HIF

Fig.7. *Measured current waveforms at PSU, calculated current approximation coefficients (Ma,Mb,Mc, Mg), differences of the sum absolute value for current detail coefficients (Ha,Hb,Hc) and approximation coefficients ratios (Ra, Rb, Rc) for different types of HIFs at 20 km from PSU at 0.04s*

For such cases, it is obvious from scheme performance in cases simulated different HIFs types that all the conditions required for recognition of HIFs are fulfilled as follows: (For example for a single line to ground HIF).

- As seen in the M-graphs of Fig.7 (a), and 7 (b), all the M-values ($Ma, Mb, and\ Mc$) are less than the threshold Mth, is achieved.
- As seen in the H-graphs of Fig.7 (a), and 7 (b), at least one of the H-values ($Ha, Hb,$ and Hc), exceeds the threshold Hth and stays above for more than 1 cycle, is also achieved.
- As seen in the R-graphs of Fig.7 (a), and 7 (b), all the R-values ($Ra, Rb,$ and Rc) are less than the threshold Rth, is also obtained.

3.4 Effect of Fault Types, Location, Inception Angle and Fault Resistance

Different fault types though out the TL length are examined with different fault types, and different inception angles. As expected, the magnitude of the maximum absolute value for current approximation coefficient (Ma, Mb, Mc) for faulted phases is much higher than the healthy phases in case of LIFs. For OCFs, additional features are used to identify these types of faults as described before.

Table 2 illustrate sample of the comprehensive carried out tests in order to demonstrate how the proposed technique is able to detect perfectly the OCFs. In all cases, the fault type is correctly detected within only one cycle after fault occurrence. Besides, different simulated switching events are examined and the PSU discriminated all as normal cases. The results prove that this proposed scheme is immune to fault locations, fault types, and different inception angles.

Table 2 Fault classifications results for various OCF types and normal switching cases

Simulated case	Location (km)	Fault resistance (Ω)	Fault inception angle, (φ°)	Maximum absolute value for approximation coefficients and Difference absolute sum value for detailed coefficients				Approximation coefficients ratios			Event classification and Fault detection time (ms)	
				$\lvert Ma\rvert \times 10^3$ $\lvert Ha\rvert \times 10^3$	$\lvert Mb\rvert \times 10^3$ $\lvert Hb\rvert \times 10^3$	$\lvert Mc\rvert \times 10^3$ $\lvert Hc\rvert \times 10^3$	$\lvert Mg\rvert$	$\lvert Ra\rvert$	$\lvert Rb\rvert$	$\lvert Rc\rvert$		
OCFTS	8	10000	36	0.0240 0.8410	0.5960 0.0070	0.6000 0.8340	0.3747×10^3	0.0403	0.9933	25.000	OCF	21.1
OCFTS	50	10000	180	0.110 0.998	0.707 0.057	0.677 0.941	0.4310×10^3	0.1556	1.0443	6.1545	OCF	21.26
OCFTS	300	10000	252	0.668 0.151	0.785 0.299	0.630 0.148	0.4851×10^3	0.8509	1.2460	0.9431	OCF	22.08
OC/R+EF Low resistance	40	10	110	0.122 0.625	0.703 0.044	0.680 0.581	0.4540×10^3	0.1735	1.0338	5.5737	OCF	24.01
OC/R+EF High resistance	310	50	146	0.700 0.140	0.781 0.359	0.609 0.219	0.5555×10^3	0.8963	1.2824	0.8700	OCF	23.64
OC/O+EF Low resistance	30	10	182	0.078 0.863	0.693 0.004	0.690 0.867	0.5118×10^3	0.11255	1.0043	8.84615	OCF	21.39
OC/O+EF High resistance	330	50	216	0.638 0.234	0.788 0.378	0.594 0.144	0.5008×10^3	0.80964	1.3269	0.9310	OCF	22.20
HIF-A	70	280	290	0.829 0.296	0.740 0.300	0.740 0.004	0.2387×10^3	1.1473	1.0000	0.87161	HIF	20.28
HIF-A	270	280	0	0.802 0.149	0.743 0.004	0.756 0.145	0.1197×10^3	1.0794	0.9828	0.94264	HIF	20.08
HIF-AB	150	280	218	0.860 0.220	0.858 0.003	0.745 0.223	0.1807×10^3	1.00233	1.1516	0.86628	HIF	21.11
HIF-AB	310	280	74	0.800	0.794	0.756	0.1132×10^3	1.00756	1.0502	0.9450	HIF	20.89

				0.119	0.094	0.225						
Mth = 0.92625×10³, Hth = 0.092625×10³ and Rth= 1.2												

3.5 CHANGING THRESHOLD VALUES ADAPTIVELY

The current waveforms, at PSU installed at the beginning of the protected line during normal load changing events (increasing at 0.1 sec and 0.2 sec), are analyzed as seen in the Fig.8(a). The threshold values are calculated adaptively using equations (3, and 4) based on the pre-fault current approximation coefficients. The differences of the sum of absolute value for current detail coefficients (Ha, Hb, Hc), and maximum absolute value for the current approximation coefficients (Ma, Mb, Mc) during such load changes are illustrated in Fig.8 (b) and 8 (c) respectively.

As displayed, no major difference in ***H-values*** happens throughout one power cycle after such normal load changes. Therefore, there is no detected fault because ***H-values*** for a more one-power cycle do not remain above threshold level. Consequently, and according to the normalized value of the adapted current approximate coefficients, the new threshold values (Mth, Hth) are updated without human interventions.

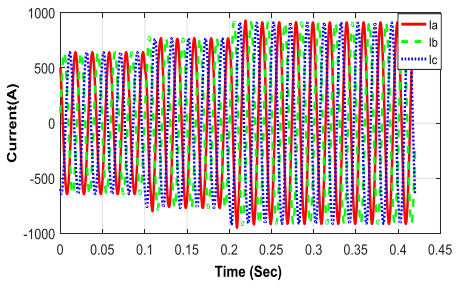

(a) Three-phase current waveforms

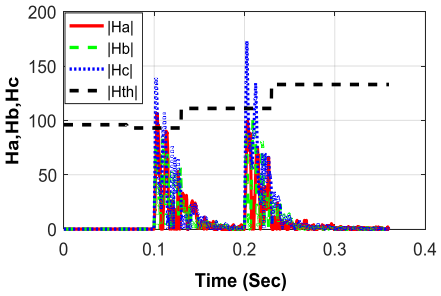

(b) Detail coefficients Ha, Hb, Hc & updated Hth

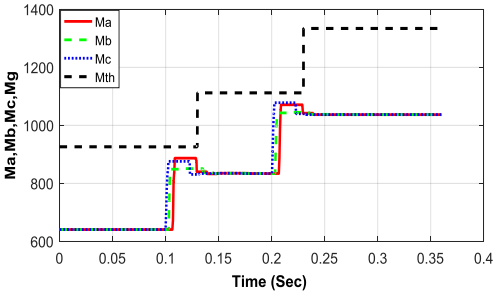

(c) Approximation coefficients Ma,Mb, Mc & updated Mth

Fig.8. *Normal load changing*

4. GENERAL PERFORMANCE EVALUATION OF PSU

From all previous test scenarios, the features of PSU can be distinguished compared with other schemes and summarized as follows:

- PSU uses only measurements taken locally. Therefore, it reduces the cost and difficulties associated with communications between two ends.
- The applied threshold values are calculated adaptively depending on the normalized value of the pre-fault current approximation coefficients.
- The logic of PSU is deterministic and no need for applying additional artificial intelligence (AI) techniques such as ANN, FLC, SVM, and KNN...etc. Hence, it avoids training for knowledge and avoids the low reliability of AI protection schemes which is highly influenced by its architecture.
- PSU has effective, reliable and robust performance, which is suitable in the case of various fault conditions, especially in the case of OCFs, and discriminate perfectly between shunt HIFs and OCFs.

5. CONCLUSIONS

Detection and location of open conductor fault (OCF) in transmission systems using single-end data is a challenging task. Actually, the protection of HV transmission systems against OCF imposes significant difficulties since OCF has a very low current undetectable by conventional distance relays. Traditionally, an OCF in transmission line (TL) may be detected by earth fault relays and cleared after a long delay time.

The paper proposes a novel single-end measuring scheme to detect and locate all kinds of open conductor faults OCFs in HV transmission systems. The proposed scheme unit (PSU) applies Discrete Wavelet Transform (DWT) with single-level decomposition on local current signals to detect OCFs, low-impedance faults (LIFs), and shunt high impedance faults (HIFs) correctly using adaptively estimated threshold values.

PSU uses current measurements from only one end of the system for fault detection and classification. That reduces cost associated with communication requirements. Low-frequency components and high-frequency components derived by DWT from current signals are used as discriminative features for detection and classification.

The achieved results denoted that the PSU can detect correctly all types of OCFs: the open conductor from two sides, the open conductor fault from one side associated with an earth fault from the other side with low or high fault resistance. Besides, PSU can also discriminate properly between LIFs, shunt HIFs and OCFs. Therefore, PSU has proved its dependability and robustness for detecting OCFs with different fault conditions.

6. REFERENCES

[1] D. I. Jeerings, J. R. Linders (1991). A Practical Protective Relay for Down-Conductor Faults, IEEE Transactions on Power Delivery, vol. 6, no. 2, pp. 565 – 574.

[2] Ebha koley, Anamika yadav, A. S. Thoke (2014). Artificial Neural Network based Protection Scheme for One Conductor Open Faults in Six Phase Transmission Line, International Journal of Computer Applications, September 2014, vol. 101, no. 4, pp. 0975 – 8887.

[3] Francisco Velez (2014). Open Conductor Analysis and Detection, IEEE PES General Meeting Conference & Exposition, National Harbor, MD.

[4] Banejad, M., Ijadi, H. (2014). High impedance fault detection: discrete wavelet transform and fuzzy function approximation, J. AI Data Mining, vol. 2, no. 2, pp. 149–158

[5] Chen, Jichao, et al. (2016). Detection of high impedance faults using current transformers for sensing and identification based on features extracted using wavelet transform, IET generation, transmission & distribution 10.12 (2016): 2990-2998.

[6] D. Guillen, M.R.A. Paternina, A. Zamora, J.M. Ramirez, G. Idarraga (2015). Detection and classification of faults in transmission lines using the maximum wavelet singular value and Euclidean norm, IET Gener. Transm. Distrib. , vol. 9, no. 15, pp. 2294–2302.

[7] D. Das, N.K. Singh, A.K. Sinha (2006). A Comparison of Fourier Transform and Wavelet Transform Methods for Detection and Classification of Faults on Transmission Lines, IEEE Power India Conference, New Delhi.

[8] C.D. Prasada, N. Srinivasua (2015). Fault Detection in Transmission Lines using Instantaneous Power with ED based Fault Index, Proced. Technol. vol. 21, pp. 132–138.

[9] N. Roya, K. Bhattacharya (). Detection, classification, and estimation of fault location on an overhead transmission line using S-transform and neural network, Elect. Power Compon. Syst. Vol. 43, no. 4, pp. 461–472.

[10] A.G. Shaik, R. Rao, V. Pulipaka (2015). A new wavelet based fault detection, classification and location in transmission lines, Electr. Power Energy Syst., vol. 64, pp. 35–40.

[11] M. Dehghani, M.H. Khooban, T. Niknam (2016). Fast fault detection and classification based on a combination of wavelet singular entropy theory and fuzzy logic in distribution lines in the presence of distributed generations, Electr. Power Energy Syst., vol. 78, pp.455–462.

[12] S. Hasheminejad, S.G. Seifossadat, M. Razaz, M. Joorabian (2016). Traveling-wave- based protection of parallel transmission lines using Teager energy operator and fuzzy systems, IET Gener. Transm. Distrib, vol. 10, no. 4, pp. 1067–1074.

[13] Sekhar, G. Chandra, and P. S. Subramanyam (2016). A logic based protection scheme for six phase transmission system against shunt and series faults", World Journal of Modelling and Simulation, vol. 12, no. 2, pp. 125-136.

[14] Swetapadma, Aleena, and Anamika Yadav (2016). Fuzzy Based Fault Location Estimation during Unearthed Open Conductor Faults in Double Circuit Transmission Line, Information Systems Design and Intelligent Applications, Proceedings of 3rd International Conference, INDIA, vol. 2, Springer, New Delhi, pp. 445-456.

[15] Rashad, Basem Abd-Elhamed, Doaa K. Ibrahim, and Mahmoud I. Gilany (2020). Adaptive single-end transient-based scheme for detection and location of open conductor faults in HV transmission lines, Electric Power Systems Research 182 (2020): 106252.

[16] Ngui, W.K, Leong, M.S, Hee. L.M, and Abdelrhmen, A.M., (2013). Wavelet analysis: Mother Wavelet Selection Methods, Applied Mechanics and Materials, Trans Tech Publications, pp. 953–958.

[17] Reddy, M.J.B., Rajesh, D.V., Mohanta, D.K., (2013). Robust transmission line fault classification using wavelet multi-resolution analysis", Comput. Electr. Eng., vol. 39, no. 4, pp. 1219–1247

[18] A.R. Adly, R.A. El Sehiemy, A.Y. Abdelaziz, and N. Ayad (2016). Critical aspects on wavelet transforms based fault identification procedures in HV transmission line", IET Generation, Transmission & Distribution, vol. 10, no. 2, pp. 508-517.